Pure Pursuit with an Effector

Alexander Von Moll[1,2*], Meir Pachter[3] and Zachariah Fuchs[2]

[1*]Control Science Center, Air Force Research Laboratory, 2210 8th St., WPAFB, 45433, OH, USA.

[2]Department of Electrical Engineering and Computing Systems, University of Cincinnati, 2600 Clifton Ave., Cincinnati, 45221, OH, USA.

[3]Department of Electrical Engineering and Computing Systems, Air Force Institute of Technology, 2950 Hobson Way, WPAFB, 45433, OH, USA.

*Corresponding author(s). E-mail(s): alexander.von_moll@us.af.mil;
Contributing authors: meir.pachter@afit.edu; fuchsze@ucmail.uc.edu;

Abstract

The study of pursuit curves is valuable in the context of air-to-air combat as pure pursuit guidance (heading directly at the target) is oftentimes implemented. The problems considered in this paper concern a Pursuer, implementing pure pursuit (i.e., line of sight guidance), chasing an Evader who holds course. Previous results are applicable to the case in which capture is defined as the two agents being coincident, i.e., point capture. The focus here is on obtaining results for the more realistic case where the pursuer is endowed with an effector whose range is finite. The scenario in which the Evader begins *inside* the Pursuer's effector range is also considered (i.e., escape from persistent surveillance, among other potential applications). Questions herein addressed include: does the engagement end in head-on collision or tail chase, will the Evader be captured or escape, what is the minimum distance the Pursuer will attain, for two Pursuers, is simultaneous capture/escape optimal and, if so, what is the optimal heading for the Evader (max time to capture, or min time to escape), and the feasibility for a fast Evader to escape from many Pursuers. Where possible,

closed-form, analytic results are obtained, otherwise attention is given to computability with an eye towards real-time, on-board implementation.

Keywords: pursuit-evasion, pure pursuit, persistent surveillance, finite capture radius

1 Introduction

The subject of one object pursuing another by aiming directly at it has long captured the imagination of mathematicians, engineers, and theoretical biologists alike. Generally, the curve traced by the Pursuer's motion is referred to as a *pursuit curve* [1, 2]. In its purported original incarnation, the problem was formulated by Bouguer as a pursuer (a pirate ship) attempting to capture an evader (a merchant ship) using Pure Pursuit (PP) [3]. It was assumed that the Evader's motion is a straight line perpendicular to the initial line of sight (LOS), i.e., a broadside or *abeam* attack. Since then, many works have been published on this problem and its many variants. Most notably, the more general case in which the Evader moves on a straight line that is *not* perpendicular to the initial LOS was only fairly recently solved in closed form by Eliezer and Barton [4, 5]. No attempt at a comprehensive survey is made here; much of the history and pertinent works are described in [6, 7][8, Chap. 3]. Nahin's book [6] re-examines the "classic" pursuit problem (in which the Evader's path is a straight line) as well as considering more complicated Evader paths (such as a circle) and cyclic pursuit (in which ring of Pursuers pursue one another). Kamimura and Ohira's book [7] contains many of the same problems as well as some three-dimensional variants (such as helical Evader paths); it also contains chapters on collective motion and group pursuit-evasion, which heavily emphasize simulation over rigorous analysis. Pure Pursuit is the subject of a full chapter in [8]; the book, which gives a general treatment of missile guidance laws, illustrates one of the important physical applications of pursuit curves, namely in air-to-air combat. One very recent, noteworthy contribution to this field is [9] wherein Gard proved that the Evader can lead a Pursuer who employs PP to any point in $\mathbb{R}^n$ while maintaining some desired minimum separation distance for the case of equal speeds. Note that the results presented herein apply to the interesting case of equal speeds.

It must also be mentioned that there is a large section of literature devoted to *game* formulations of pursuit-evasion. This includes works pertaining to fast evaders as well as multiple pursuers, both of which are analyzed in this paper under the assumption that the Pursuers employ PP. Of course, pursuit-evasion was one of the main flavors of example within Isaacs' book on differential games [10] wherein a candidate solution was presented for the two-Pursuer pursuit-evasion game of min max capture time with point capture. Concerning evasion from many pursuers, many works have analyzed different varations

including the work by Pshenichnyi [11], Chikrii [12], in addition to the excellent review of the subject by Kumkov *et al.* [13]. As for games with a faster Evader, the classic work by Hagedorn and Breakwell [14] solves a game wherein the Evader must pass between two Pursuers who seek to approach as close as possible. The work of Chernous'ko [15] contains an important result which states that a fast Evader can avoid point capture by any number of slower Pursuers via an arbitrarily small deviation from its prespecified straight-line path. This result, in particular, highlights the need to consider non-point capture in the context of a faster Evader. Finally, works such as those by Ramana and Kothari [16] and Garcia and Bopardikar [17] consider a faster Evader against Pursuers who cooperate by trying to enclose the former within some formation.

Much of the existing work on PP has been focused on the case in which the Evader's path is a straight line and capture occurs when the Pursuer and Evader are coincident (point capture) [2, 4, 5, 8]. This paper continues in a similar vain but with a focus on non-point capture; that is, the Pursuer may effect capture within some specified distance. This paper pertains to pursuit-evasion scenarios taking place in an unbounded, obstacle-free two-dimensional environment, i.e., the realistic plane. The agents' speeds are fixed and non-zero. It is assumed throughout that the Evader implements a constant heading (holds course) in the inertial (global) Cartesian frame – in some cases, the Evader heading is assumed to be given, and in others it may be considered to be a decision made at the initial time instant. The Pursuer(s) strategy is PP; in the case of multiple Pursuers, the speeds are assumed to be equal, however the results in this paper can be readily extended to the unequal speed case and/or the unequal effector range case. The Pursuer(s) may be endowed with an effector of radius l. Table 1 lists the different scenarios considered; μ is the ratio of Evader and Pursuer speeds and d_0 is the initial distance between the agents. Scenario 4, "Escape from surveillance", is distinct from the other scenarios in that the Evader begins *inside* the Pursuer's effector range and termination is said to occur when the Evader is able to maneuver beyond the Pursuer's range. There is no notion of capture in this Scenario. In this case, the Pursuer's effector may be thought of as some kind of sensor which the Evader would like to avoid.

Table 1 Taxonomy of Pursuit-Evasion Scenarios; μ is the ratio of Evader and Pursuer speeds, l is the Pursuer's effector range, and d_0 is the initial separation distance between the agents.

#	Setting			Description
1	$\mu < 1$	$l = 0$	$d_0 > 0$	Point Capture
2	$\mu < 1$	$l > 0$	$d_0 > l$	Capture (slow Evader)
3	$\mu > 1$	$l > 0$	$d_0 > l$	Capture (fast Evader)
4	$\mu > 1$	$l > 0$	$d_0 < l$	Escape from surveillance

The contributions of this work are as follows (with parentheses indicating to which Scenario(s) the result applies). Aspect angle refers to the angle that the Evader's heading makes w.r.t. the Pursuer's LOS.

- Solution for the Pursuer's separation distance as a function of aspect angle (1–4)
- Analytic determination of head-on versus tail-chase final configuration (2, 3)
- Necessary and sufficient condition for capture/evasion (3)
- Solution for capture time (2, 3) and escape time (4)
- Proof of the existence of a solution for simultaneous capture (1)
- Necessary condition for simultaneous capture (1, 2) and escape (4)
- Sufficient condition for simultaneous capture (2)

Insomuch as is possible, the results are closed-form, analytic expression. Otherwise, attention is given to numerical implementation.

The remainder of the paper is organized as follows. Section 2 specifies the problem setup. Section 3 provides the analysis leading to the determination of the final configuration. Section 4 contains the results pertaining to final time (i.e., when capture or escape occurs). Section 5 examines the case where there are two Pursuers wherein simultaneous capture (or escape) is possible. Finally, Section 6 contains the conclusion.

2 Preliminaries

Let the agents' positions be specified by $E \equiv (x_E, y_E)$ and $P \equiv (x_P, y_P)$, $E, P \in \mathbb{R}^2$. In the case that there are $M > 1$ Pursuers, the ith Pursuer position is denoted P_i, where $i \in 1, \ldots, M$. Without loss of generality, the Pursuer(s')

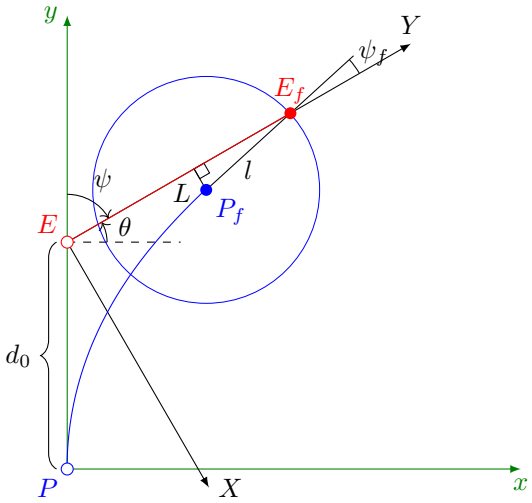

Fig. 1 Schematic illustration of the scenario corresponding to Scenario 2: slow Evader and finite capture radius.

speed is fixed to 1 and the Evader's speed is μ. Additionally, w.l.o.g., consider a Cartesian frame (x, y) whose origin is the Pursuer's initial position and whose positive y-axis is aligned with the line segment $\overline{PE}$ at initial time (the green axes in Fig. 1)[1]. The kinematics, which arise from P employing the strategy of PP are

$$\begin{bmatrix} \dot{x}_E \\ \dot{y}_E \\ \dot{x}_P \\ \dot{y}_P \end{bmatrix} = \begin{bmatrix} \mu \cos(\theta) \\ \mu \sin(\theta) \\ \frac{x_E - x_P}{d} \\ \frac{y_E - y_P}{d} \end{bmatrix} \tag{1}$$

where $d \equiv \sqrt{(x_E - x_P)^2 + (y_E - y_P)^2}$ is the instantaneous distance between the agents, and θ is the Evader's heading angle w.r.t. the positive x-axis. The Pursuer's effector range is l – in the case of capture, this corresponds to the capture radius; in the case of surveillance, this corresponds to observation range. Final time, t_f, is defined as the time at which the distance between P and E is equal to the effector range, i.e., $d(t_f) = l$.

The rotated Cartesian frame, (X, Y), (shown in black in Fig. 1) is used here in the expression of the so-called *pursuit curve* [2]. In this frame, the origin is the Evader's position at the initial time and the Y-axis is aligned with the Evader's (constant) direction of motion, or course. The kinematics in this frame are

$$\begin{bmatrix} \dot{X}_E \\ \dot{Y}_E \\ \dot{X}_P \\ \dot{Y}_P \end{bmatrix} = \begin{bmatrix} 0 \\ \mu \\ -\frac{X_P}{\sqrt{X_P^2 + (Y_E - Y_P)^2}} \\ \frac{Y_E - Y_P}{\sqrt{X_P^2 + (Y_E - Y_P)^2}} \end{bmatrix}. \tag{2}$$

Two useful expressions are given by Barton and Eliezer, namely the tangent function [2]

$$\frac{\mathrm{d}Y_P}{\mathrm{d}X_P} = \frac{1}{2}\left(w \left(\frac{X_P}{X_{P_0}} \right)^{\mu} - \frac{1}{w} \left(\frac{X_P}{X_{P_0}} \right)^{-\mu} \right), \tag{3}$$

and the solution of P's trajectory [2]:

$$\begin{aligned} Y_P(X_P) = {} & \frac{\mu X_{P_0}(1 + \mu \sin\theta)}{\cos\theta(1 - \mu^2)} + \\ & \frac{X_{P_0}}{2}\left[\frac{w}{1+\mu} \left(\frac{X_P}{X_{P_0}} \right)^{1+\mu} - \frac{1}{w(1-\mu)} \left(\frac{X_P}{X_{P_0}} \right)^{1-\mu} \right], \end{aligned} \tag{4}$$

where $w \equiv \frac{1 - \sin\theta}{\cos\theta}$ and $X_{P_0} \equiv X_P(t_0) = d_0 \cos\theta$. Note that, at all time, the tangent to the Pursuer's trajectory points to E, by construction [2, 8].

There are two cases for which (4) does not apply: 1) when $\theta = \pm\frac{\pi}{2}$, and 2) when $\mu = 1$. First, when $\theta = \pm\frac{\pi}{2}$, the Evader is moving directly away or towards the Pursuer, respectively. Either way, (4) is ill-defined (as the first

[1] We utilize this convention in some portions of the text to match the work of [2].

term goes to infinity) but also unnecessary as the scenario plays out entirely on the one-dimensional line passing through the two agents. Second, when $\mu = 1$, the last term in the bracket goes to infinity. However, by substituting $\mu = 1$ into (3) and integrating, a specialized pursuit curve expression may be obtained[2]:

$$Y_P(X_P) = -X_{P_0} \tan\theta + \frac{wX_{P_0}}{4}\left(\left(\frac{X_P}{X_{P_0}}\right)^2 - 1\right) - \frac{X_{P_0}}{2w}\log\left(\frac{X_P}{X_{P_0}}\right). \quad (5)$$

The transformation to the (x, y) frame is

$$\begin{bmatrix} x_P \\ y_P \end{bmatrix} = \begin{bmatrix} \sin\theta & \cos\theta \\ -\cos\theta & \sin\theta \end{bmatrix} \begin{bmatrix} X_P \\ Y_P \end{bmatrix} + \begin{bmatrix} 0 \\ d_0 \end{bmatrix}. \quad (6)$$

Lastly, consider a rotating frame which is defined by the distance from P to E and E's heading w.r.t. P's line of sight. The kinematics (which are obtained by inspection of Fig. 1) are

$$\begin{bmatrix} \dot{d} \\ \dot{\psi} \end{bmatrix} = \begin{bmatrix} \mu\cos\psi - 1 \\ -\frac{\mu}{d}\sin\psi \end{bmatrix} \quad (7)$$

where, w.l.o.g., $\psi \in [0, \pi]$. The term ψ is referred to as the aspect angle, and is generally not constant even though the Evader's heading is constant in the inertial frame (unless $\psi = 0$). It is clear, with the convention for ψ, that $\dot{\psi} < 0$ for all t since $\sin\psi > 0$ and $d > 0$. This monotonicity holds whether the Evader is slow or fast. Regarding distance, d, if the Evader is slow ($\mu < 1$) then $\dot{d} < 0$ for all t which means the Pursuer is always getting closer; but if the speed ratio $\mu > 1$ then there is a range of ψ for which $\dot{d} > 0$.

Proposition 1 *A Pursuer remains on the same half-plane in which it started w.r.t. the Evader's heading and initial position.*

Proof In order for the Pursuer to cross into the opposite half-plane there must be a time at which $\psi = 0$. It is clear from (7) that $\dot{\psi} = 0$ and thus the Pursuer will remain in a trailing configuration as long as the Evader holds course (i.e., P never crosses into the opposite half-plane). □

It is for this reason that we restrict our attention to the range $\psi \in [0, \pi]$.

[2]This had been left as an exercise to the reader in [2]. It can be shown, using (9) that the distance asymptotically approaches $\frac{d_0(\cos\psi_0+1)}{2}$.

3 Final Configuration

Before addressing the determination of final time for a particular problem instance, it is important to determine whether the Evader has a component of velocity *towards* or *away* from the Pursuer at final time, i.e., whether the scenario ends in a head-on or tail-chase configuration. To do this, we obtain the solution of (7). First, divide the two differential equations:

$$\begin{aligned}\frac{\mathrm{d}d}{\mathrm{d}\psi} = \frac{\dot{d}}{\dot{\psi}} &= \frac{\mu\cos\psi - 1}{-\frac{\mu}{d}\sin\psi} \\ &= \frac{d\left(\frac{1}{\mu} - \cos\psi\right)}{\sin\psi},\end{aligned} \tag{8}$$

which can be simplified as follows

$$\begin{aligned}\frac{1}{d}\mathrm{d}d &= \left(\frac{1}{\mu\sin\psi} - \frac{1}{\tan\psi}\right)\mathrm{d}\psi \\ \int_{d_0}^{d_f}\frac{1}{d}\,\mathrm{d}d &= \int_{\psi_0}^{\psi_f}\frac{1}{\mu\sin\psi}\,\mathrm{d}\psi - \int_{\psi_0}^{\psi_f}\frac{1}{\tan\psi}\,\mathrm{d}\psi \\ [\ln d]_{d_0}^{d_f} &= -\frac{1}{\mu}\left[\ln\left(\cot\psi + \csc\psi\right)\right]_{\psi_0}^{\psi_f} - \left[\ln\left(\sin\psi\right)\right]_{\psi_0}^{\psi_f} \\ \ln d_f - \ln d_0 &= -\frac{1}{\mu}\ln\left(\cot\psi_f + \csc\psi_f\right) \\ &\quad + \frac{1}{\mu}\ln\left(\cot\psi_0 + \csc\psi_0\right) \\ &\quad - \ln\sin\psi_f + \ln\sin\psi_0.\end{aligned}$$

Taking the exponential of both sides gives

$$\mathrm{e}^{\ln d_f - \ln d_0} = \mathrm{e}^{-\frac{1}{\mu}\ln(\cot\psi_f + \csc\psi_f) + \frac{1}{\mu}\ln(\cot\psi_0 + \csc\psi_0) - \ln\sin\psi_f + \ln\sin\psi_0},$$

which becomes

$$\begin{aligned}\frac{\mathrm{e}^{\ln d_f}}{\mathrm{e}^{\ln d_0}} &= \mathrm{e}^{-\frac{1}{\mu}\ln(\cot\psi_f + \csc\psi_f)}\mathrm{e}^{\ln\frac{1}{\mu}(\cot\psi_0 + \csc\psi_0)}\frac{\mathrm{e}^{\ln\sin\psi_0}}{\mathrm{e}^{\ln\sin\psi_f}} \\ \frac{d_f}{d_0} &= \left(\cot\psi_f + \csc\psi_f\right)^{-\frac{1}{\mu}}\left(\cot\psi_0 + \csc\psi_0\right)^{\frac{1}{\mu}}\frac{\sin\psi_0}{\sin\psi_f},\end{aligned}$$

which can be rearranged to

$$d_f\left(\cot\psi_f + \csc\psi_f\right)^{\frac{1}{\mu}}\sin\psi_f = d_0\left(\cot\psi_0 + \csc\psi_0\right)^{\frac{1}{\mu}}\sin\psi_0. \tag{9}$$

This expression is the solution of the system (7). Given the initial and final aspect angle and either distance, (9) yields a closed-form, analytic solution for

the unknown distance. Unfortunately, if either ψ_0 or ψ_f is unknown, then (9) must be solved numerically.

Proposition 2 *The curve*

$$d_\perp(\psi_0;\, l, \mu) = l\left(\cot\psi_0 + \csc\psi_0\right)^{-\frac{1}{\mu}} \csc\psi_0 \tag{10}$$

partitions the state space into a region of Pursuer initial positions, (d_0, ψ_0)*, which end in head-on collision* $(\cos\psi_f < 0)$*, and a region for which the scenario ends in a tail-chase* $(\cos\psi_f > 0)$*. More precisely:*

$$\operatorname{sign}\left(\cos\psi_f\right) = \begin{cases} -1 & \text{if } d_0 < d_\perp \\ \text{undef.} & \text{if } d_0 = d_\perp \\ 1 & \text{if } d_0 > d_\perp. \end{cases} \tag{11}$$

Proof Substituting $d_f = l$ and $\psi_f = \frac{\pi}{2}$ into (9) immediately gives (10). This configuration corresponds to the Evader's heading being perpendicular to the Pursuer's at the moment that $d \to l$, which is the case that is neither head-on collision nor tail-chase. If $\psi_f = \frac{\pi}{2}$ then $\cos\psi_f = 0$, hence $\operatorname{sign}\left(\cos\psi_f\right)$ is undefined as in (11). The remainder of the proof is broken into two cases depending on the magnitude of μ.

Slow Evader

in this case, $\mu < 1$ and both ψ and d are monotonically decreasing w.r.t. time. Thus, if, for the same ψ_0, $d_0 < d_\perp$, the Pursuer must take a shorter time to capture the Evader. Since ψ is monotonic, it must be the case that $\psi_f > \frac{\pi}{2}$ which implies that $\cos\psi_f < 0$. The case where $d_0 > d_\perp$ follows by similar logic.

Fast Evader

in this case, $\mu > 1$ and only ψ is monotonically decreasing w.r.t. time. From (7), it is clear that

$$\operatorname{sign}(\dot{d}) = \begin{cases} -1 & \text{if } \cos\psi < \frac{1}{\mu} \\ 0 & \text{if } \cos\psi = \frac{1}{\mu} \\ 1 & \text{if } \cos\psi > \frac{1}{\mu}. \end{cases}$$

Therefore, the distance becomes monotonically *increasing* once $\cos\psi > \frac{1}{\mu}$. Capture, if it occurs at all, must take place while $\cos\psi < \frac{1}{\mu}$. Thus capture can only occur in the portion of the trajectory for which d is monotonically decreasing. Because of this, the same logic used to prove the case where $\mu < 1$ can be applied to this case as well. □

Remark 1 For the escape from surveillance scenario (Scenario 4), the final configuration is always tail-chase because for E to escape the observation range of P it must have $d_f = l$ and $\dot{d}_f > 0$, which means $\cos\psi_f > \frac{1}{\mu} > 0$.

Proposition 3 *For the fast Evader capture scenario* $(\mu > 1,\ d_0 > l)$*, the curve*

$$d_{c/e}(\psi_0;\, l, \mu) = l\left(\cot\psi^\dagger + \csc\psi^\dagger\right)^{\frac{1}{\mu}} \sin\psi^\dagger \cdot \left(\cot\psi_0 + \csc\psi_0\right)^{-\frac{1}{\mu}} \csc\psi_0, \tag{12}$$

where

$$\psi^{\dagger} \equiv \cos^{-1} \frac{1}{\mu}, \tag{13}$$

partitions the state space into a region of Pursuer initial positions, (d_0, ψ_0)*, which end in capture and a region for which evasion occurs. In the latter case,* $t_f \to \infty$*,* $\psi \to 0$*, and* $d \to \infty$*. Stated differently,* $d_0 < d_{c/e}$ *is a necessary and sufficient condition for capture.*

Proof Two things are necessary for capture: the first is that the distance from E to P is equal to the latter's effector range, l, and the second is that P is actually *closing* in on E (i.e., $\dot{d} < 0$). If $d = l$ but $\dot{d} \geq 0$ then the Evader is escaping since d will increase monotonically from there on out. This is akin to Isaacs' notion of the *Usable Part* (UP) of the terminal surface [10].

The limiting case for escape occurs when $\dot{d} = 0$, which, from (7) occurs when $\psi = \psi^{\dagger}$. For any $\psi < \psi^{\dagger}$ it would be the case that $\dot{d} > 0$. Then (12) follows directly from substituting $d_f = l$ and $\psi_f = \psi^{\dagger}$ into (9). The fact that $d_0 < d_{c/e}$ is required follows from monotonicity arguments akin to those in the proof of Proposition 2. □

Proposition 4 *Ignoring termination, the minimum inter-agent distance in the fast Evader case* $(\mu > 1)$ *is*

$$d_{\min}(d_0, \psi_0;\ \mu) = d_0 \left(\cot\psi_0 + \csc\psi_0\right)^{\frac{1}{\mu}} \sin\psi_0 \cdot \left(\cot\psi^{\dagger} + \csc\psi^{\dagger}\right)^{-\frac{1}{\mu}} \csc\psi^{\dagger}, \tag{14}$$

if $\psi_0 > \psi^{\dagger}$*, and* $d_{\min} = d_0$ *otherwise.*

Proof Eq. (14) is obtained by substituting $d_f = d_{\min}$ and $\psi_f = \psi^{\dagger}$ into (9). This corresponds to the minimum distance because, from (7) $\dot{d} = 0$ when $\psi = \psi^{\dagger}$ and the fact that d is monotonically decreasing while $\psi > \psi^{\dagger}$ and monotonically increasing while $\psi < \psi^{\dagger}$. If $\psi < \psi^{\dagger}$, then d is monotonically decreasing and thus the minimum distance is the current distance. □

Corollary 1 *For the fast Evader capture scenario* $(\mu > 1,\ d_0 > l)$*, the capture condition,* (12)*, is equivalent to* $d_{\min} < l$*.*

Proof The result follows directly from Propositions 2–4. □

Following are some examples which illustrate the aforementioned curves and regions for both the slow and fast Evader scenarios. In all of these examples, the Evader's heading is aligned with the positive x-axis. Fig. 2 shows the curve $d_{\perp}$ for a slow Evader along with example tail-chase and head-on Pursuer trajectories. Then Fig. 3 shows a similar plot, but for a fast Evader; additionally, the curve $d_{c/e}$ is shown. In the case where P begins outside the capture region (labeled "Miss Example"), the trajectory is shown up to the time at

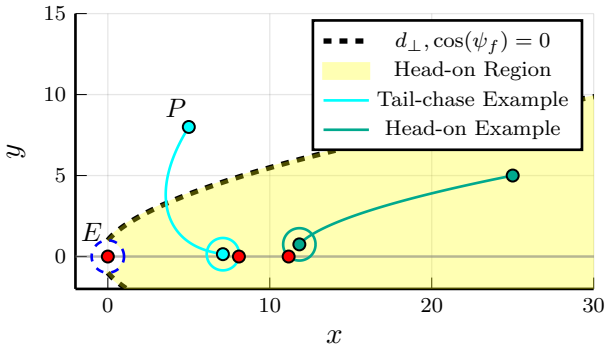

Fig. 2 Slow Evader example; $\mu = 0.8$, $l = 1$.

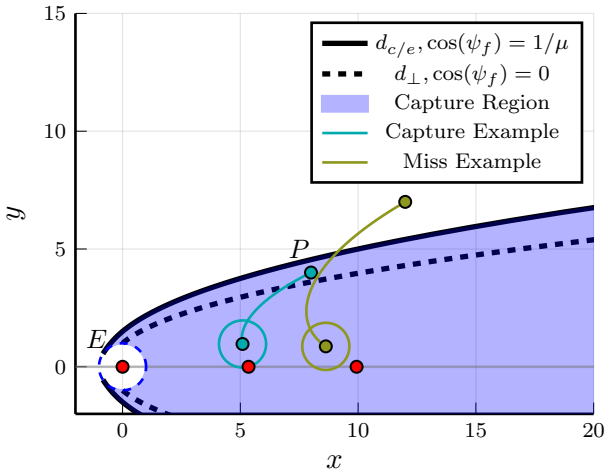

Fig. 3 Fast Evader example; $\mu = 1.2$, $l = 1$.

which $d = d_{\min}$. Finally, Fig. 4 shows a map of $d_{\min}$ as a function of P's initial position.

4 Final Time

In this section, the final time, t_f, associated with each of the scenarios is characterized. The final configuration is an important component in the determination of the final time in the case of non-point capture ($l > 0$). For point capture, however, there is no need to make a distinction between head-on and tail-chase; indeed the capture time for a slow, fixed-course Evader and point capture is well-known, appearing in [2, 8, 18] and many other places. Given the pursuit curve in (4), the final time associated with Scenario 1 is found by substituting in $X_{P_f} = 0$ and $Y_{E_f} = Y_{P_f}$ and noting that E travels from

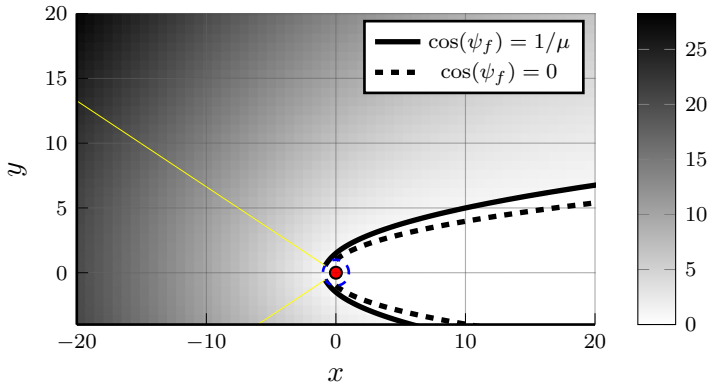

Fig. 4 Miss distance as a function of P's initial position; $\mu = 1.2$, $l = 1$. The yellow lines mark out a cone inside which $d_{\min} = d_0$.

$(X_E, Y_E) = (0, 0)$ to $(0, Y_{E_f})$ in t_f time at speed μ. Thus,

$$\begin{aligned} t_f &= \frac{Y_{E_f}}{\mu} = \frac{Y_P\left(X_P = 0\right)}{\mu} \\ &= \left(\frac{1 + \mu \sin\theta}{1 - \mu^2}\right) d_0 \end{aligned} \tag{15}$$

In Scenarios 2–4 the Pursuer's effector range is $l > 0$. Let the final lateral separation in the Evader-aligned frame, (X, Y), be defined as $X_{P_f} \equiv L$ (see Fig. 1). As in every other point along P's trajectory, the line-of-sight $\overline{P_f E_f}$, is tangent to the pursuit curve, $Y_P(X_P)$ [8]. This observation leads to a derivation for L as follows:

$$\begin{aligned} \tan\psi_f &= \left.\frac{\mathrm{d}X_P}{\mathrm{d}Y_P}\right|_{t=t_f} \\ \cot\psi_f &= \left.\frac{\mathrm{d}Y_P}{\mathrm{d}X_P}\right|_{t=t_f} \\ \frac{\sqrt{1 - \sin^2\psi_f}}{\sin\psi_f} &= \\ \frac{l\sqrt{1 - \frac{L^2}{l^2}}}{L} &= \\ l^2\left(1 - \frac{L^2}{l^2}\right) &= L^2\left(\left.\frac{\mathrm{d}Y_P}{\mathrm{d}X_P}\right|_{t=t_f}\right)^2 \\ l^2 - L^2 &= \end{aligned}$$

$$\implies L = \frac{l}{\sqrt{1 + \left(\frac{\mathrm{d}Y_P}{\mathrm{d}X_P}\big|_{t=t_f}\right)^2}}. \tag{16}$$

Evaluating (3) at $X_P = L$ and substituting into the above gives

$$\begin{aligned} L &= \frac{l}{\sqrt{1 + \frac{1}{4}\left[w^2\left(\frac{L}{X_{P_0}}\right)^{2\mu} + \frac{1}{w^2}\left(\frac{L}{X_{P_0}}\right)^{-2\mu} - 2\right]}} \\ &= \frac{l}{\sqrt{\frac{1}{4}\left[w^2\left(\frac{L}{X_{P_0}}\right)^{2\mu} + \frac{1}{w^2}\left(\frac{L}{X_{P_0}}\right)^{-2\mu} + 2\right]}} \\ \implies L &= \frac{2l}{w\left(\frac{L}{X_{P_0}}\right)^{\mu} + \frac{1}{w}\left(\frac{L}{X_{P_0}}\right)^{-\mu}} \end{aligned} \tag{17}$$

Proposition 5 *For $d_0 > l > 0$, $\mu < 1$ (i.e., Scenario 2), (17) has a unique solution on the interval $L \in [0, \min\{d_0 \cos\theta, l\})$.*

Proof Concerning the range for the solution, we must have $L < l$ because $L > l$ would require P being further from E than the capture radius. Also, it must be the case that $L = X_{P_f} < X_{P_0} = d_0 \cos\theta$ because $X_P(t)$ is monotonically decreasing (which follows from the fact that P is employing the strategy PP) and $d_0 > l$. Two conditions were used to derive (17): (*i*) $d_f = l$ and (*ii*) the tangency equation, (3), is satisfied. The latter is true by construction, since P is always aiming at E's instantaneous position. As for the former, if $d_0 > l$, then at some point it must be the case that $d = l$ because d is monotonically decreasing when $\mu < 1$ (see (7)). Additionally, there can only be one such instance, again, because of d's monotonicity. Therefore, a solution to (17) exists and is unique. □

Proposition 6 *For $d_0 > l > 0$, $\mu > 1$ (i.e., Scenario 3), (17) has a unique solution on the interval $L \in [0, \min\{d_0 \cos\theta, l\})$ if and only if $d_0 < d_{c/e}$.*

Proof When $d_0 < d_{c/e}$, capture must occur due to Proposition 3. The distance between P and E must be monotonically decreasing along the entire trajectory since, in order for capture to be possible, $\psi > \psi^\dagger$ for all t. Therefore, by similar arguments as in the preceding proof, the premise must be true. □

Proposition 7 *For $d_0 < l$, $\mu > 1$ (i.e., Scenario 4), (17) has a unique solution on the interval $L \in [0, \min\{d_0 \cos\theta, l\})$.*

Proof As in Scenario 3, d is monotonically decreasing w.r.t. time while $\psi > \psi^\dagger$ and monotonically increasing thereafter. Since $d_0 < l$, eventually there must be a time at which $d = l$, and this instance must be unique, and, as in previous proofs, this implies that (17) is satisfied. □

Remark 2 When $0 < L \ll 1$, (17) suffers from some numerical instability due to the $(L/X_0)^{-\mu}$ term. This is often the case for Scenario 4, especially when μ is close to 1. In this case, it is generally easier to numerically solve (9) for ψ_f and then compute $L = l \sin \psi_f$.

In the general case, since the solution of L exists and is unique, any root finding method is suitable for its computation. However, in some special circumstances, as shown in the following, the problem structure may be further exploited to aid in the computation of L.

Proposition 8 *If either (i) $d_0 > l$ and E can be captured or (ii) $d_0 < l$ with $\mu > 1$, and the speed ratio μ is a rational number (that is, $\mu = \frac{r}{q}$ where $r, q \in \mathbb{N}^+$), then the solution of (17) may be obtained via the rooting of a polynomial.*

Proof Define $\mathscr{L} \equiv \left(\frac{L}{X_{P_0}}\right)^{\frac{1}{q}}$ and substitute into (17)

$$\mathscr{L}^q X_{P_0} = \frac{2l}{w\mathscr{L}^r + \frac{1}{w}\mathscr{L}^{-r}}$$

$$\implies \mathscr{L}^{q+r} X_{P_0} w + \mathscr{L}^{q-r} X_{P_0} \frac{1}{w} - 2l = 0. \tag{18}$$

Thus $\mathscr{L}$ may be obtained as the solution of a $(q + r)$th-order (sparse) polynomial, and the associated final lateral separation is $L = \mathscr{L}^q X_{P_0}$. □

If, for example, the speed ratio is $\mu = \frac{1}{2}$, it comes down to solving a cubic equation.

Proposition 9 *For $d_0 > l > 0$ (i.e., Scenarios 2 and 3), the time to capture (if E can be captured) is*

$$t_f = \frac{1}{\mu}\left(Y_P(L) + \operatorname{sign}(d_0 - d_\perp)\sqrt{l^2 - L^2}\right), \tag{19}$$

where L is obtained as the solution of (17), and Y_P is given by (4).

Proof As in the point capture case, the final time is found by substituting the final conditions into the pursuit curve, (4), and observing that E traverses a distance Y_{E_f} in t_f time:

$$t_f = \frac{Y_{E_f}}{\mu} = \frac{1}{\mu}\left(Y_{P_f} \pm \sqrt{l^2 - L^2}\right).$$

The $\pm$ in the above expression is due to the fact that $Y_{E_f} - Y_{P_f}$ can be positive or negative. In the case of tail-chase, $Y_{E_f} - Y_{P_f} > 0$, and *vice versa* for head-on collision. Recall, from Proposition 2 (particularly (11)), that the question of final configuration is determined by whether $d \lessgtr d_\perp$. Hence, the sign $(d_0 - d_\perp)$ term in (19) yields the proper sign for $Y_{E_f} - Y_{P_f}$. □

Proposition 10 *For $d_0 > l > 0$ (i.e., Scenarios 2 and 3), the time to capture (if E can be captured) is bounded above by*

$$\bar{t} = \begin{cases} (15) & \text{if } \mu < 1 \\ \frac{1}{\mu}\left(Y_P\left(d_{\min}\sin\psi^\dagger\right) + \text{sign}(d_0 - d_\perp)\frac{d_{\min}}{\mu}\right) & \text{if } \mu > 1 \end{cases}, \tag{20}$$

where Y_P is given by (4), $d_{\min}$ is given by (14), and $\psi^\dagger$ is given by (13).

Proof For $\mu < 1$, the distance, d, is always decreasing monotonically, so since $l > 0$, the time to capture (i.e., (19)) must be less than the time to drive $d \to 0$, which is given by the point capture time, (15). For $\mu > 1$, the distance, d, is always decreasing monotonically until $\psi = \psi^\dagger$ (as described in the proof of Proposition 4). The premise is that capture is possible, so $d_{\min} < l$ from Corollary 1, so, again, the time to capture must be less than the time to drive $d \to d_{\min}$. □

This upper bound on capture time may be especially useful in the context of engagements between many agents wherein computational complexity becomes a concern. For example, a particular Evader may only need to consider the one or two Pursuers with the smallest upper bound, after which a more precise computation may be performed (similar to how certain Pursuers could be ignored in [19]). Additionally, for $\mu < 1$, the minimum upper bound, $\min_i \bar{t}_i$, provides an upper bound on the value of the game of min max capture time (c.f. [20]).

Corollary 2 *For $d_0 < l$, $\mu > 1$ (i.e., Scenario 4), the time to capture is*

$$t_f = \frac{1}{\mu}\left(Y_P(L) + \sqrt{l^2 - L^2}\right), \tag{21}$$

where L is obtained as the solution of (17), and Y_P is given by (4).

Proof The proof is similar to the preceding proofs. Eq. (21) is a specialization of (19) since the final configuration is always tail-chase for Scenario 4. This is because, for escape, it must be the case that $\dot{d}_f > 0$, otherwise E is *entering* P's effector range. Since $\mu > 1$, we must have $\psi_f < \psi^\dagger$ in order for $\dot{d}_f > 0$, and since $\psi^\dagger < \frac{\pi}{2}$, this must be a tail-chase configuration. □

Using (19), the capture loci (i.e., the final Evader position, $E_f(\psi_0)$) are plotted for various effector ranges, l, in Fig. 5. As expected, as the Pursuer's effector range increases, the locus shrinks towards E's initial position. The curve corresponding to $l = 0$ is obtained analytically via (15). A similar figure appears in [8, Fig. 3.6], but for point capture with varying speed ratios.

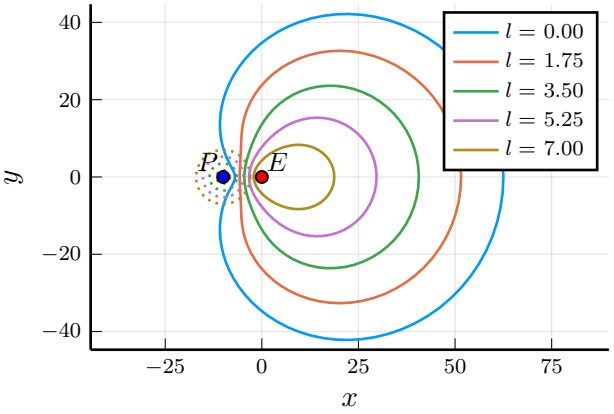

Fig. 5 Capture loci (final E positions) for constant-heading Evader trajectories for varying effector ranges, l; here $\mu = 0.8$.

5 Simultaneous Capture and Escape

In this section, a second Pursuer is considered whose speed is equal to that of the first Pursuer[3]; the problem setup is shown in Fig. 6 (note that $\alpha \in \left[0, \frac{\pi}{2}\right]$). For Scenarios 1 and 2, it is assumed that E wishes to delay capture for as long as possible while employing a constant-heading strategy. The point capture version of this problem has been analyzed, e.g., in [18]. A finite-capture-range version was treated in [21], however, there, the Evader was not constrained to a constant heading and its optimal control was computed (i.e., $\max_{\theta(t)} t_f$). For capture by a single Pursuer, E's optimal heading was indeed constant (Pure Evasion (PE), in fact). However, in the case of simultaneous capture by both Pursuers, E's optimal heading was not constant (except when E's position is on the bisector of the angle $\angle P_1 E P_2$). The solution developed here thus provides a lower bound for the optimal capture time, which, as will be shown, requires far less computation than the optimal, in general. Note that the solution for the differential game version of the two-Pursuer problem with finite capture range is given in [22]. For Scenario 3, conditions for the existence of an evasive heading are developed, which readily extend to the case of many Pursuers. For Scenario 4, it is assumed that E wishes to escape from within the Pursuers' effector range in minimum time. The single-Pursuer case with P implementing $\arg\max_{u_P(t)} t_f$ is solved in [23]. To summarize, the Evader's optimal control is defined as

$$\hat{\theta}^* \equiv \begin{cases} \arg\max_{\hat{\theta}} t_f(\hat{\theta}) & \text{for Scenarios 1–3,} \\ \arg\min_{\hat{\theta}} t_f(\hat{\theta}) & \text{for Scenario 4 (escape).} \end{cases} \tag{22}$$

As always, the two Pursuers implement PP.

[3] Unequal Pursuer speeds can also be handled by keeping track of, e.g., μ_1 and μ_2 throughout the derivation, and similarly for unequal effector ranges via l_1 and l_2.

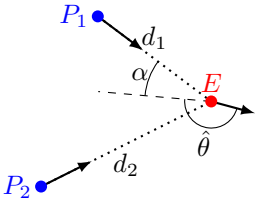

Fig. 6 Schematic illustration of the two-Pursuer problem.

Let t_{f_1} and t_{f_2} be defined as the times at which $d_1 = l$ and $d_2 = l$, respectively. Obviously, whether we are considering capture or escape, simultaneity implies that $t_{f_1} = t_{f_2}$. Also define $\hat{\theta}^*$ as the associated optimal Evader heading for each Scenario, where $\hat{\theta}$ is the Evader's heading measured w.r.t. the angular bisector between the Pursuers. Furthermore, define α as the half-angle between the Pursuers (c.f. Fig. 6).

Proposition 11 *The optimal Evader heading for Scenarios 1–4 lies in the range* $\hat{\theta}^* \in [\pi - \alpha, \pi + \alpha]$.

Proof In all Scenarios, E must try to make $\dot{d}_1$ and $\dot{d}_2$ as large as possible. Headings outside the stated range are worse for both distance rates than headings within the range. A similar argument is given in [21] and analyzed in more detail there. □

It may be the case that one or other Pursuer is sufficiently far such that they have no effect on the outcome. Then, it is always best for E to employ the strategy PE against the nearer Pursuer, as in [21]. The following Theorems establish conditions under which simultaneous capture is optimal. They are based on checking if, while employing the strategy PE from a Pursuer, the other Pursuer captures E first. Define the hypothetical single-Pursuer capture time associated with PE as

$$t_{i_{PE}} = \left| \frac{d_i - l}{1 - \mu} \right|, \qquad i = 1, 2. \tag{23}$$

Theorem 1 *For* $l = 0$, $\mu < 1$ *(i.e., Scenario 1), simultaneous capture is optimal iff*

$$t_{1_{PE}} > t_{f_2}(\hat{\theta} = \pi - \alpha) \text{ and } t_{2_{PE}} > t_{f_1}(\hat{\theta} = \pi + \alpha), \tag{24}$$

which simplifies to

$$\frac{1 + \mu \cos(2\alpha)}{1 + \mu} < \frac{d_1}{d_2} < \frac{1 + \mu}{1 + \mu \cos(2\alpha)}. \tag{25}$$

Proof First, we require (24) because, otherwise, it would be optimal to be captured by only one Pursuer (c.f. [21]). Substituting (15) and (23) (with $l = 0$) into the first

condition gives

$$\frac{d_1}{1-\mu} > \left(\frac{1-\mu\cos\left(\hat{\theta}-\alpha\right)}{1-\mu^2}\right) d_2$$

$$\frac{d_1}{d_2} > \frac{1+\mu\cos(2\alpha)}{1+\mu}$$

A similar substitution for the second condition yields the inverse of this expression. Hence (25) must be satisfied in order for simultaneous capture to be optimal. □

Note, an expression similar to (25) appears in the two-Pursuer differential game version of the problem wherein the Pursuers select their instantaneous headings so as to minimize capture time [24].

Theorem 2 *For $l = 0$, $\mu < 1$ (i.e., Scenario 1), if (25) is satisfied, then the (unique) optimal Evader heading is*

$$\hat{\theta}^* = \sin^{-1}\left(\frac{d_2 - d_1}{\mu d_1 C}\right) - \gamma, \tag{26}$$

where

$$\sin\gamma = \left(\frac{d_2}{d_1} - 1\right)\frac{\cos\alpha}{C}, \qquad \cos\gamma = \left(\frac{d_2}{d_1} + 1\right)\frac{\sin\alpha}{C}, \tag{27}$$

and

$$C = \sqrt{\frac{d_2^2}{d_1^2} + 1 + 2\frac{d_2}{d_1}\left(1 - 2\cos^2\alpha\right)}. \tag{28}$$

Proof Theorem 1 says that simultaneous capture is optimal since (25) is satisfied. Thus there must be a $\hat{\theta}^*$ for which $t_{f_1} = t_{f_2}$. Define $\theta_1 = \frac{3\pi}{2} - \hat{\theta} - \alpha$ and $\theta_2 = \hat{\theta} - \frac{\pi}{2} - \alpha$. Substituting them into (15) and setting the capture times equal gives

$$\left(\frac{d_2}{d_1} - 1\right)\cos\hat{\theta}\cos\alpha + \left(\frac{d_2}{d_1} + 1\right)\sin\hat{\theta}\sin\alpha = \frac{d_2 - d_1}{\mu d_1}.$$

Then, dividing by C, using the definition for γ, (27), and the angle sum identity, gives (26). Moreover, the solution is unique because t_{f_1} and t_{f_2} are monotonically decreasing and increasing, respectively, over the range specified in Proposition 11 (which can be easily shown by taking the derivative of t_{f_1} and t_{f_2} w.r.t. $\hat{\theta}$). □

The process is the same as above for Scenario 2, where $l > 0$.

Corollary 3 *For $l > 0$, $\mu < 1$ (i.e., Scenario 2), simultaneous capture is optimal iff*

$$\begin{aligned} t_{1_{PE}} &> t_{f_2}(\hat{\theta} = \pi - \alpha; \quad l > 0), \\ t_{2_{PE}} &> t_{f_1}(\hat{\theta} = \pi + \alpha; \quad l > 0). \end{aligned} \tag{29}$$

However, the computation of $t_{f_1}(\hat{\theta} = \pi + \alpha)$ and $t_{f_2}(\hat{\theta} = \pi - \alpha)$ is more difficult (in that it requires the solution of (17)). A more computationally efficient check involves making use of the capture time associated with point capture at the cost of being a weaker condition.

Theorem 3 *For $l = 0$, $\mu < 1$ (i.e., Scenario 2), simultaneous capture is optimal if*

$$\frac{1+\cos(2\alpha)}{1+\mu} < \frac{d_1 - l}{d_2 - l} < \frac{1+\mu}{1+\cos(2\alpha)}. \tag{30}$$

Note, this condition is sufficient, but not necessary.

Proof First, note that the capture time associated with $l > 0$ must be less than the capture time for $l = 0$ from Proposition 10. So, instead of checking for PE against Pursuer i and computing the actual capture time for Pursuer j, the closed-form, analytic expression for the point capture case, (15), may be used. Since $t_{f_{l=0}} > t_{f_{l>0}}$, it is sufficient to show that $t_{i_{PE}} > t_{f_{j,l=0}}$ for $i, j \in \{1, 2\}$, $i \neq j$. Then (30) is obtained similarly as in the proof of Theorem 1. □

Fig. 7 shows, for particular Pursuer positions, the regions for which conditions (29) and (30) are satisfied. The sufficient region covers much of the simultaneous capture region, especially for Evader positions near the Pursuers.

For Scenario 3, the situation is somewhat different since there is a range of headings for which the Evader can guarantee evasion against a particular Pursuer. In the event that E has no safe headings to take when there are two Pursuers, then Corollary 3 applies. The interesting feature of this case thus becomes the Evader's range of safe headings. Recall that the limiting case for capture when $\mu > 1$ corresponds with $\psi_f = \psi^\dagger$ and $d_f = l$ since this corresponds to the minimum distance (c.f. 4). Then, given the initial position of P and E, the safe range of Evader headings is given by $\Psi_s \equiv [-\psi_s, \psi_s]$,

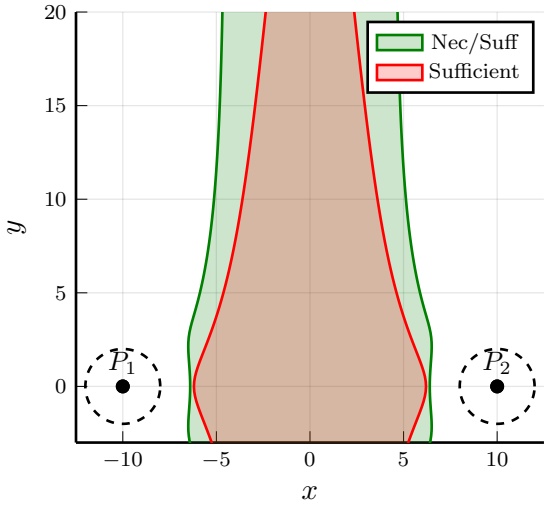

Fig. 7 Example coverage of the sufficient condition, (30), compared to the necessary and sufficient condition, (29); the Pursuer positions are fixed and the regions correspond to possible Evader positions, $\mu = 0.8$ and $l = 2$.

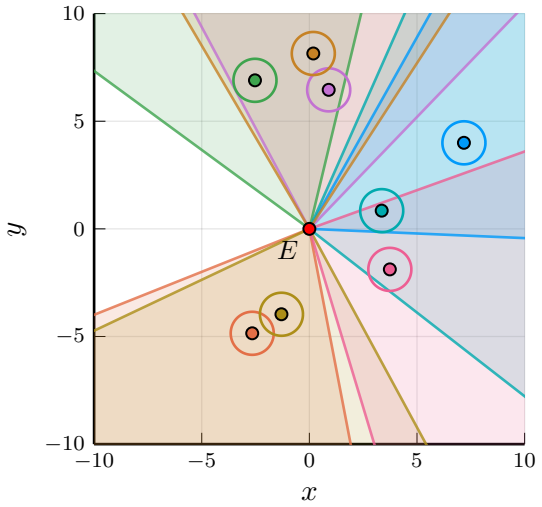

Fig. 8 Fast capture example with many Pursuers in which the safe range of Evader headings (shown as the clear cone) is nonempty. For the purposes of visualization, the complement of Ψ_{s_i} is shown. Here, $\mu = 1.2$ and $l = 1$.

where ψ_s is the (numerical) solution of (9). If there are *many* Pursuers, the safe range associated with each Pursuer, Ψ_{s_i}, may be computed, and the overall safe range is given by their intersection:

$$\Psi_s = \cap_{i=1}^{M} \Psi_{s_i}. \tag{31}$$

Of course, if $\Psi_s = \emptyset$, then capture is guaranteed. Fig. 8 shows an example with $M = 8$ Pursuers in which the overall safe range, Ψ_s, is nonempty. The Evader need only choose a heading in the clear region in order to guarantee evasion.

Finally, for Scenario 4, recall that the Evader seeks to minimize the amount of time it takes to drive $d > l$; the necessary and sufficient condition for the optimality of simultaneous escape is as follows.

Corollary 4 *For $l > 0$, $\mu > 1$ (i.e., Scenario 4), if $d_1, d_2 < l$ then simultaneous escape is optimal iff*

$$\begin{aligned} t_{1_{PE}} &< t_{f_2}(\hat{\theta} = \pi - \alpha;\ l > 0), \\ t_{2_{PE}} &< t_{f_1}(\hat{\theta} = \pi + \alpha;\ l > 0). \end{aligned} \tag{32}$$

Unlike in Scenario 2 there is no obvious relaxation of this condition, since point capture is not generally possible when $\mu > 1$. The general case in which E is inside the effector range of one Pursuer but outside the other's is more complex, hence, above it is assumed that E is within l of both Pursuers. Fig. 9 shows an example of simultaneous escape.

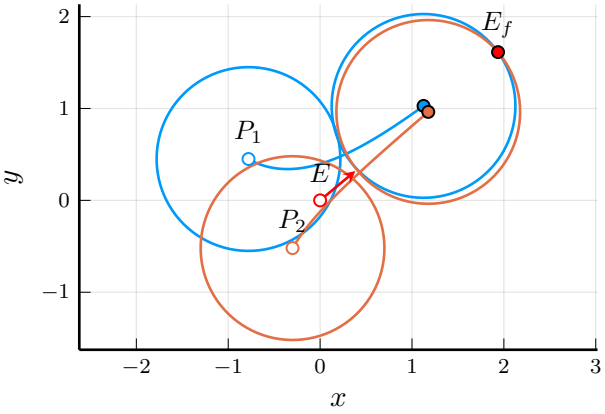

Fig. 9 Simultaneous escape example with the numerically computed optimal Evader heading; $\mu = 1.2$ and $l = 1$.

6 Conclusion

In this paper, we have extended the results for the classical pursuit-evasion problem into the realm of non-point capture. These results are thus one step closer to real-world situations, such as air-to-air combat, wherein a missile armed with a proximity fuse need only come within some finite distance to destroy its target. The curves governing the final configuration (tail-chase or head-on) and whether capture happens (for a speed ratio $\mu > 1$) were obtained in closed form. An analytic expression for the minimum distance attained by the Pursuer was also derived. The final time for finite effector range ($l > 0$) may be obtained via any standard root-finding method, or (for rational μ) as the rooting of a sparse polynomial. Some of the results were applied directly to the wolf pack scenario of many-on-one, i.e., $M \geq 2$ Pursuers. Another possible extension is to utilize the safe range for Evader headings as a constraint in an Evader path planning algorithm. Lastly, the scenario of escape from persistent surveillance with multiple Pursuers is a rich area for further development.

Acknowledgments. This paper is based on work performed at the Air Force Research Laboratory (AFRL) *Control Science Center*. Distribution Unlimited. 16 Feb 2022. Case #AFRL-2022-0728.

Declarations.

Funding. This work has been supported in part by AFOSR LRIR No. 21RQCOR084.

Conflict of interest. Not applicable

Ethics Approval. Not applicable

Consent to participate. Not applicable

Consent for publication. Not applicable

Availability of data and materials. This article has no associated data or materials.

Code availability. This article has no associated code.

Authors contributions. A. Von Moll prepared the manuscript, developed theoretical results, and produced the examples. M. Pachter developed the algorithm for computing finite-capture-radius capture time and aided in the analysis. Z. Fuchs contributed to the analysis as well.

References

[1] Boole, G.: A Treatise on Differential Equations. A Treatise on Differential Equations, vol. v. 1. Macmillan, London (1872)

[2] Barton, J.C., Eliezer, C.J.: On pursuit curves. The Journal of the Australian Mathematical Society. Series B. Applied Mathematics **41**, 358–371 (2000). https://doi.org/10.1017/S0334270000011292

[3] Bouguer, P.: Lignes de poursuite. Mémoires de l'Académie Royale des Sciences (1732)

[4] Eliezer, C.J., Barton, J.C.: Pursuit curves. Bulletin of the Institute of Mathematics and its Applications **28**, 182–184 (1992)

[5] Eliezer, C.J., Barton, J.C.: Pursuit curves ii. Bulletin of the Institute of Mathematics and its Applications **31**, 139–141 (1995)

[6] Nahin, P.J.: Chases and Escapes. Princeton University Press, New Jersey (2012). https://doi.org/10.1515/9781400842063

[7] Kamimura, A., Ohira, T.: Group Chase and Escape. Theoretical Biology. Springer, Singapore (2019). https://doi.org/10.1007/978-981-15-1731-0_2

[8] Shneydor, N.A.: Missile Guidance and Pursuit: Kinematics, Dynamics and Control. Woodhead Publishing, Sawston, UK (1998)

[9] Gard, A.: The wild goose chase problem. The American Mathematical Monthly **125**, 602–611 (2018). https://doi.org/10.1080/00029890.2018.1465785

[10] Isaacs, R.: Differential Games: A Mathematical Theory with Applications to Optimization, Control and Warfare. Wiley, New York (1965)

[11] Pshenichnyi, B.N.: Simple pursuit by several objects. Cybernetics **12**, 484–485 (1976). https://doi.org/10.1007/BF01070036

[12] Chikrii, A.A., Prokopovich, P.V.: Simple pursuit of one evader by a group. Cybernetics and Systems Analysis **28**, 438–444 (1992). https://doi.org/10.1007/BF01125424

[13] Kumkov, S.S., Le Ménec, S., Patsko, V.S.: Zero-sum pursuit-evasion differential games with many objects: Survey of publications. Dynamic Games and Applications **7**, 609–633 (2017). https://doi.org/10.1007/s13235-016-0209-z

[14] Hagedorn, P., Breakwell, J.V.: A differential game with two pursuers and one evader. Journal of Optimization Theory and Applications **18**, 15–29 (1976). https://doi.org/10.1007/BF00933791

[15] Chernous'ko, F.L.: A problem of evasion from many pursuers. Journal of Applied Mathematics and Mechanics **40**, 11–20 (1976). https://doi.org/10.1016/0021-8928(76)90105-2

[16] Ramana, M.V., Kothari, M.: Pursuit-evasion games of high speed evader. Journal of Intelligent & Robotic Systems **85**, 293–306 (2017). https://doi.org/10.1007/s10846-016-0379-3

[17] Garcia, E., Bopardikar, S.D.: Cooperative containment of a high-speed evader. In: 2021 American Control Conference (ACC). IEEE, New Orleans, LA, USA (2021). https://doi.org/10.23919/acc50511.2021.9483097

[18] Makkapati, V.R., Sun, W., Tsiotras, P.: Optimal evading strategies for two-pursuer/one-evader problems. Journal of Guidance, Control, and Dynamics **41**, 851–862 (2018). https://doi.org/10.2514/1.G003070

[19] Von Moll, A., Casbeer, D., Garcia, E., Milutinović, D., Pachter, M.: The multi-pursuer single-evader game: A geometric approach. Journal of Intelligent and Robotic Systems **96**, 193–207 (2019). https://doi.org/10.1007/s10846-018-0963-9

[20] Von Moll, A., Pachter, M., Garcia, E., Casbeer, D., Milutinović, D.: Robust policies for a multiple pursuer single evader differential game. Dynamic Games and Applications, 202–221 (2019). https://doi.org/10.1007/s13235-019-00313-3

[21] Von Moll, A., Fuchs, Z., Pachter, M.: Optimal evasion against dual pure pursuit. In: American Control Conference. IEEE, Denver, CO (2020). https://doi.org/10.23919/ACC45564.2020.9147776

[22] Pachter, M., Wasz, P.: On a two cutters and fugitive ship differential game. IEEE Control Systems Letters **3**, 913–917 (2019). https://doi.org/10.1109/lcsys.2019.2919418

[23] Weintraub, I.E., Von Moll, A., Garcia, E., Casbeer, D., Demers, Z.J.L., Pachter, M.: Maximum observation of a faster non-maneuvering target by a slower observer. In: American Control Conference, Denver, CO (2020). https://doi.org/10.23919/ACC45564.2020.9147340

[24] Pachter, M., Von Moll, A., Garcia, E., Casbeer, D., Milutinović, D.: Two-on-one pursuit. Journal of Guidance, Control, and Dynamics **42**(7) (2019). https://doi.org/10.2514/1.G004068